DR-1089

CONF-741105-8

Distribution Category UC-20

PLASMA CONFINEMENT IN THE OGRA-3 SIMPLE MIRROR TRAP IN THE PRESENCE OF A MULTI-ELEMENT FEEDBACK SYSTEM

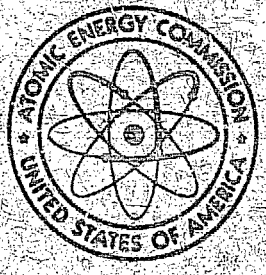

UNITED STATES ATOMIC ENERGY COMMISSION
Office of Information Services
Technical Information Center

This is a translation of paper CN-33/D-4 from the 5th Conference on Plasma Physics and Controlled Nuclear Fusion Research, Tokyo, Japan, November 11-15, 1974, prepared by the Foreign Resources Associates, Fort Collins, Colorado. This translation was funded by the USAEC Division of Controlled Thermonuclear Research.

In the interest of expeditious dissemination, this publication has been reproduced directly from copy prepared by the translating agency.

Printed in USA. Price $4.00. Available from the National Technical Information Service, U. S. Department of Commerce, Springfield, Virginia 22161.

Issuance Date: December 1974.

Printed in the United States of America
USAEC Technical Information Center, Oak Ridge, Tennessee

PLASMA CONFINEMENT IN THE OGRA-3 SIMPLE MIRROR TRAP IN THE PRESENCE OF A MULTI-ELEMENT FEEDBACK SYSTEM

V. A. Zhil'tsov, V. Kh. Likhtenshteyn, D. A. Panov, P. M. Kosarev, V. A. Chuyanov, and A. G. Shcherbakov

I. V. Kurchatov Institute of Atomic Energy, Moscow, USSR

ABSTRACT

The Ogra-3 apparatus is a simple magnetic mirror trap with a 2.1 mirror ratio and central magnetic field of up to 25 kG, specially constructed for conducting investigations into plasma stabilization with the aid of feedback circuits. Plasma is obtained within the Ogra-3 via injection into a vacuum of a beam of hydrogen atoms with energy of 20 kev and intensity greater than 50 equiv. mA. The vacuum conditions assure a lifetime of around 0.1 sec before charge exchange for the fast ions captured in the trap. Without special measures being taken, the plasma within the Ogra-3 is unstable with respect to hydromagnetic flute oscillations, which restrict plasma build-up near the instability threshold at densities of $1\text{-}2\cdot10^{8}$ cm^{-3}.

An electrostatic, 12-electrode feedback system with Fourier dimensional synthesis (analysis) was created to stabilize the flute instability; it suppresses the lower space modes of flute instability.

By using it we were able to raise the threshold density of the onset of loss 10-fold and observe excitation and stabilization of the higher modes of flute instability.

Experiments with the 12-electrode system showed that the previously detected drop in losses at positive transfer coefficients of the feedback system is not a result of stabilization of flute instability, but rather is associated with nonlinear effects (namely, with a drop in the phase velocities of unstable waves and a reduction in their interaction with the confined fast ions). At the same time, these experiments demonstrated the existence of a region of stability for negative transfer coefficients. This region of stability was predicted theoretically, but was not observed in early experiments with stabilizing systems having a small number of stabilizing electrodes.

An investigation was conducted and a comparison was made with the theory of plasma dispersion properties in the presence of a feedback system. In accordance with the theoretical predictions, three branches of flute oscillations were detected and their change under the influence of feedback was studied.

INTRODUCTION

The Ogra-3 simple mirror trap with injection of fast hydrogen atoms is specially intended for continuing the investigation into stabilization of plasma flute instability by feedback systems [1-4]. Physical experiments in this apparatus were instituted in the autumn of 1972, and their initial results were published in [5].

In the simple mirror field of the Ogra-3 the plasma is unstable with respect to hydromagnetic flute oscillations, which also restrict density build-up near its onset threshold ($n_0 \approx 10^8$ cm^{-3}). The experiments described in [5] showed that the introduction of feedback with the aid of external electrodes makes it possible to somewhat raise the onset threshold of losses from the trap, this rise depending on the number of independent feedback loops (electrodes) employed. The loss threshold receives a 3-3.5-fold increment with the maximum number of electrodes (4), with the greatest effect being achieved when the amplification factor of the feedback system is positive. Density build-up does not exceed 50% with negative feedback.

A theoretical analysis of stabilizing systems with a finite number of stabilizing electrodes conducted simultaneously with the experiments in [5] showed that, in contrast to the distributed stabilizing systems examined earlier [1,2], the determining effect for systems with a finite number of electrodes is modal interaction, which sharply constricts the region of stability. Moreover, solutions derived for actual configurations of sensing elements and electrodes showed that the boundary condition adopted in [1] and subsequent works which is introduced by the feedback system

$$\varphi_w = \delta \cdot \varphi_s \qquad (1)$$

(here, φ_s is the plasma surface potential r = a, φ_w is wall potential r = b regulated by the feedback system, and δ is the transfer coefficient) does not correspond to the actual method for incorporating feedback and should be replaced by

$$\varphi_w = - \frac{\partial \varphi(r)}{\partial r} \cdot \delta \cdot b \qquad (2)$$

The change in the boundary condition results in stability becoming theoretically possible only with negative transfer coefficients, in contrast to [1], in which theory predicted regions of stability for both signs of feedback. Numerical calculations showed that with four stabilizing electrodes and negative feedback the threshold of instability cannot be raised by more than 50% due to interaction of azimuthal modes. The observed density increment with positive feedback evidently is a non-linear effect associated with a decrease in losses for a reduction in the real portion of the flute oscillation frequency under the influence of feedback [3]. According to this analysis, the achievement of stability over a wide range of densities can be anticipated only with a considerable increase in the number of stabilizing electrodes.

Thus, the theory and preceding experiment [3] pointed to the necessity of conducting experiments with a rather large number of feedback electrodes. It therefore was decided to conduct the experiments with a 12-electrode feedback system. With this number of elements the effects of modal interaction for mode m = 1 become insignificant (mode m = 1 proves to be related to modes 11 and 13 by coupling coefficient 10^{-3}, and the coupling with higher modes is on the order of 10^{-6}), and the total range of stability with an accounting of all azimuthal modes should undergo an approximately 5-fold expansion in the most pessimistic predictions. Thus, the 12-electrode system should make it possible to carry out for the first time a reasonably reliable comparison of experiments with the theory behind the analytical study.

II. Experimental apparatus and diagnostics

The magnetic field of the Ogra-3 with intensity of up to 24 kG is created by a superconducting magnet [6]. The mirror ratio equals 2.1, and mirror spacing equals 44 cm. In the median plane the field decreases in radius in conformity to the parabolic law:

$$B = B_0 \left(1 - \beta r^2 \right)$$

with the decrease factor $\beta = 2.22 \cdot 10^{-3}$.

Plasma build-up is accomplished with an injector of fast hydrogen atoms with energy of 20 keV [7]. This injector provides an equivalent current of fast atoms of up to 0.4 A through the 10×20-cm^2 input aperture of the trap. In the experiments described below, however, the input aperture was artificially limited by elements of the stabilizing system to 4×6 cm^2, and the injected current accordingly did not exceed 50 equiv. mA. The measured capture factor of the injected beam on the magnetic field with fields of 20-21 kG in a volume with radius of 8 cm was $1\text{-}4 \cdot 10^{-4}$ depending on the thickness of the magnesium target on which charge exchange of the proton beam occurs within the injector.

The vacuum conditions within the trap provided a fast proton lifetime before charge exchange of around 0.2 sec at low injection currents. At maximum injected currents the gas lifetime remained not worse than 0.1-0.05 sec.

The following methods, which have already become traditional in similar types of investigations, were used for diagnosing the resulting plasma. Plasma density averaged by volume was determined according to the flow of fast charge-exchange atoms recorded by a foil detector. Axial distribution of density was measured by a multi-commutator-segment, secondary-emission detector of fast charge-exchange atoms. Radial distribution of density was found according to flows of slow ions emerging behind the mirrors along the magnetic field lines of force. Measurement of the energy of these ions by a multi-element probe provided information on plasma potential. The energy distribution of the confined particles was measured by a 5-circuit electrostatic analyzer of fast charge-exchange atoms. A pulsed charge-exchange target was used to make these methods of corpuscular diagnostics insensitive to dynamic changes in the vacuum during the injection pulse: a beam of thermal tin atoms was passed through the plasma with intensity modulated at frequencies from 5 to 1000 Hz. Introduction of such a charge-exchange target with known density makes it possible to measure plasma density independently according to the amplitude of the variable component in the signal from the corpuscular detectors, and to determine neutral gas pressure within the plasma according to the relation of the variable portion of the signal to a constant.

Electrostatic pscillations of the plasma were recorded over the 0-2-MHz range, and over the 10-200-MHz range with the use of a great number of electrostatic probes located both at different points along the azimuth around the plasma and on different radii from the side of the plasma. These electronics made it possible to conduct Fourier dimensional analysis of low-frequency signals and separated the amplitudes of the first 4 azimuthal modes.

III. Stabilization system

The stabilization system (Fig. 1) consists of 12 electrodes uniformly positioned over a cylindrical surface with radius of 6.5 cm. Each of the electrodes occupies 1/12 of the circumference. Interelectrode gaps equal 1 mm. The length of the electrodes along the magnetic field is 10 cm. Apertures scaled to beam size are made in the corresponding electrodes in the median plane of the trap for beam injection. The 12 electrostatic sensing elements are removed 6 cm from the central plane along the magnetic field and placed as the electrodes uniformly around the plasma. The azimuths of the centers of the sensing elements and the electrodes coincide. The size of each sensing element is 0.8 × × 1.5 cm^2. The sensing elements had to be removed from the central plane in order to free the area for beam injection. This results in a drop in sensing element sensitivity by a factor of 5 and a corresponding increase in the required amplification in the feedback circuit. Each sensing element could simply have been connected to the corresponding stabilizing electrode through an amplifier, as was done earlier. However, the large number of sensing elements allowed us to employ a different feedback system: signals from all sensing elements feed into a Fourier analysis unit, where they are totaled with the appropriate Fourier coefficients and from them are formed the sine and cosine components A_m and B_m. Analyzers for the first 4 modes are now operating in the system. The accuracy of the analysis is such that in the m = 2 circuit only 1/25 of the m = 1 signal is present and vice versa. From the Fourier-synthesis unit the signals are fed into a shaping unit, and also are used for diagnostic purposes. The shaping units make it possible to select the optimum amplification and frequency characteristic of feedback independently for each mode. The fact that the sine and cosine components of

the signal are shifted 90° out of phase makes it possible, summarizing these signals, to introduce a phase shift independent from frequency. From the shaping units the amplitudes of each mode are fed to 12 summator-synthesizers, where they are summarized with all equal Fourier coefficients in order to synthesize the signal of each stabilizing electrode. Each summator-synthesizer is connected through an amplifier with its own stabilizing electrode. The maximum signal amplitude on the electrodes is 300 V from peak to peak. The frequency band in the circuits of the different modes varies and is specially selected for the experiment. The initial "basic" band of the general elements in the channel is 50 Hz to 500 kHz.

A similar "non-local" feedback system, besides the obvious advantages associated with the flexibility of independent control of stabilization parameters for the diverse modes and convenience of diagnostics, also gives a substantial advantage over noises and stray currents, and eases the conflict with system self-excitation since it completely squelches input signals that have a simultaneous cophasal effect on all inputs.

It is obvious that the sensing elements are sensitive not only to the plasma discharge fields, but also the field of the stabilizing electrodes. This spurious feedback results in a limitation on amplification and self-excitation on the decays of the frequency characteristic for a negative transfer coefficient. In order to avoid these effects, this feedback system is augmented by positive feedback circuits (not shown in Fig. 1) between the electrodes and sensing elements, which compensate for the coupling through the volume occupied by the plasma. The accuracy of this compensation is 5% over the whole frequency band. Thanks to this scheme, in the theoretical analysis it can be assumed that the sensing elements are sensitive solely to the field of plasma discharges.

IV. Experimental results

As was expected, with the use of the 12-electrode stabilizing system a drop in losses was observed for both the positive and negative feedback phases. Whereas the expansion of the region of stability with positive feedback was insubstantial in comparison with the 4-electrode

system, with negative feedback the region of stability grew by almost an order of magnitude. Fig. 2 shows mean plasma density as a function of the product of injection current times gas lifetime for negative feedback and a varied number of stabilized modes. Switching on stabilization of the first mode results in a rise in the threshold of onset of losses from 1 to $4 \cdot 10^8$ cm^{-3}. Oscillations of the m = 2 azimuthal mode emerge at this density. Losses are clearly correlated with the appearance of oscillations of the second mode. Switching on the m = 2 mode stabilizing circuit results in a further rise in density to $9 \cdot 10^8$ cm^{-3}. At this density m = 3 mode oscillations begin. At present, however, experiments in stabilization of mode m = 3 are still not complete and we cannot state unequivocally that the losses are associated strictly with this mode, because at the same time residual oscillations of the m = 1 mode also are observed. A series of experiments was conducted with a simplified stabilizing system without modal separation with each sensing element being connected directly to the appropriate stabilizing electrode. With this system it was impossible to select the optimum conditions for stabilizing each mode because the action was felt immediately on all modes. In this case the loss threshold was slightly above $1.1 \cdot 10^9$ cm^{-3}. Further development of the stabilization system and introduction of m = 3, 4, and 5 circuits will demonstrate whether it is possible to rise to higher levels or if the observed limitation is associated with causes other than higher azimuthal modes, e.g., higher radial modes.

With negative feedback not only was the region of stability broader, but the "quality" of stabilization was higher. Figure 3 shows plasma potential as a function of its density for negative and positive feedback phases. It is evident that electron containment is substantially better with the negative phase than the positive. With positive feedback, plasma decompensation exceeds 50%. It is possible that in this consists the mechanism of non-linear stabilization of plasma with positive feedback.

A drop in potential results in elimination of axial plasma expansion. The axial distributions of density are shown in Fig. 4. It is

evident that with negative feedback the half-width of the distribution is practically unchanged with a rise in density, and even at moderate density of $3 \cdot 10^8$ is only half as good as with positive feedback. At maximum densities the half-width of distribution with negative feedback is smaller than with positive feedback by a factor of 5.

Plasma in the Ogra-3 is unstable not only with respect to flute oscillations, but also with respect to oscillations on cyclotron frequencies. Oscillations on the cyclotron frequency appear at densities around 2-4·10^7 cm^{-3}, i.e., below the threshold of flute oscillations. They do not restrict build-up, however, and with a density increment the unstable frequencies pass into the higher cyclotron harmonics. Here each harmonic is unstable only over a narrow density range. If density rises rather quickly, then the cyclotron oscillations do not have a substantial effect on the plasma. When stabilization of flute oscillations is switched on, the half-width of the function of fast particle energy distribution does not exceed 30%. But if there is no stabilization and density is limited to around 10^8 in the band of severe oscillations on harmonics 1 and 2, then the effect of broadening becomes considerable. It should be noted. however, that that stated about the minor role of cyclotron oscillations holds true only for rather strong magnetic fields. For fields below 15-17 kG losses due to cyclotron oscillations become noticeable; therefore, all the described experiments were conducted with a field of 21.6 kG.

Low-frequency oscillations and the losses associated with them are very sensitive to phase shifts in the feedback system. In order for all intrinsic oscillations to be damped, a very complex shape of frequency characteristic is required, which depends on plasma density, its potential, and other parameters. Under build-up conditions, when plasma density varies by more than one order of magnitude, these conditions can be satisfied only with automatic tuning of the stabilization system parameters. Our experiments did not have this as their goal. Since the greatest losses are associated with oscillations on frequencies near the ion precession frequency [3], we strove to suppress the ionic branch of flute oscillations. This can be achieved [2] by raising the

frequency characteristic on the high frequencies (forcing) or by introducing an advancing phase shift that does not depend on frequency. If in the region of the precession frequency (in our case 70 kHz) the frequency characteristic is falling, then an intensive oscillation is observed at 70 kHz, restricting plasma density to a level below $1 \cdot 10^8$ cm^{-3}. Figure 5 shows plasma density and frequencies of low-frequency oscillations of the m = 1 mode as functions of an advancing phase shift not dependent on frequency with a falling frequency characteristic. Similar dependences are observed with the introduction of a phase shift dependent on frequency with the aid of forcing of the frequency characteristic. The experimental results described in this report were obtained with a falling frequency characteristic and advancing shift of 45° (Fig. 5).

The pattern corresponding to Fig. 5 is observed only at rather high amplification factors in the feedback system. With low amplification, oscillations with frequencies above the precession frequency are not present. Figure 6 shows the frequency of high-frequency oscillations of the m = 1 mode as a function of the amplification factor at fixed density. It is evident that there is a precise threshold of appearance of high frequencies. The value of threshold amplification corresponds with 50% accuracy to the calculation carried out on the basis of measurements of sensing element sensitivity and eq. 4 (cf. below).

The density dependence of the observed frequencies of mode m = 1 oscillations is illustrated in Fig. 7. All of the waves shown in Fig. 7 propagate in the direction of the magnetic drift of the ions. It is convenient to divide the observed frequencies into two classes: low (below the ion precession frequency of 70 kHz) and high (above 70 kHz). At least three low-frequency branches are observed, which at maximum densities merge into the practically white spectrum of oscillations. A high-frequency branch is observed only with rather high amplifications and experiences the characteristic division at high density, with that density at which division occurs greatly depending on the feedback system parameters. It should be noted that in the undivided section high-frequency branches for high oscillation amplifications are observed with small phase shifts of both signs, i.e., build-up of this branch is not connected with dissipative effects, but rather is hydrodynamic.

V. Discussion

A large number of stabilizing electrodes and use of Fourier dimensional synthesis (analysis) make it possible to make a comparison of the results for mode m = 1 with a theoretical model constructed for the distributed feedback system. For a plasma with parabolic distribution of density along a radius, the dispersion equation can be written in the form [8]:

$$\varkappa^2 = -\frac{2\omega_{oi}\cdot m}{\omega_{Bi}\cdot a^2}\left(\frac{1}{\omega} - \frac{1}{\omega + m\omega^*}\right) \qquad (3)$$

where ω^* is the ion precession frequency, ω_{oi} is ionic plasma frequency, ω_{Bi} is the ion cyclotron frequency, a is plasma radius, and $\varkappa$ is the characteristic radial wave number, which with an accounting of boundary condition (2) and compensation for spurious feedback between electrodes and sensing elements is determined by the equation:

$$\frac{J_{|m|}(\varkappa a)}{J_{|m+1|}(\varkappa a)} = \frac{\varkappa a}{2|m|}\left[1 - \left(\frac{a}{b}\right)^{2|m|} + K\right] \qquad (4)$$

Here, K is the transfer coefficient of a feedback system with electrodes located on radius b determined by the correlation:

$$K = \left(\frac{a}{b}\right)^{2|m|}\cdot\frac{|m|}{b}\cdot\frac{\varphi_w}{E_r} \qquad (5)$$

$E_r = -\frac{\partial\varphi}{\partial r}$ is the electrical field acting on the sensing element. φ_w is the potential of the stabilizing electrode. Thus, in eq. (2) $\delta = K\cdot\left(\frac{a}{b}\right)^{2|m|}\cdot\frac{1}{|m|}$

Equation (4) has an infinite set of real solutions to which the different radial modes of oscillations correspond. For $K < 0$ and with an increase in modulus $|K|$, the value of $\varkappa a$ rises and according to (3) the stability threshold rises. However, for $K \to \infty$ the value of the first root of $\varkappa a$ cannot exceed the asymptotic value of 5, 136, since here the field outside the plasma vanishes and the feedback system

cannot learn of the appearance of oscillations. The results of solution of system (3) and (4) for K = 0 (curve 1) and asymptotic values of the first and second roots of eq. (4) (curves II and IV) are given in Fig. 7. In calculating curves II and IV, a correction was inserted in eq. (4) for the effect of the final Larmor radius [9,10], which in our case of $\rho/a = 0.18$ becomes substantial and somewhat raises the instability threshold. As is evident from Fig. 7, the first low-frequency branch that we observed corresponds to the first radial mode with asymptotic value of $\varkappa a$. Good agreement here is not surprising since for high amplifications the asymptotic value only slightly depends on the feedback parameters. The following low-frequency branches evidently can be ascribed to higher radial modes, taking into consideration the possibility of deviation of the shape of radial density distribution from the parabolic.

According to eq. (3), at densities greater than $3.2 \cdot 10^8$ cm^{-3} oscillations for asymptotic values of $\varkappa a$ should be neutrally stable, and at greater densities flute instability should appear at a frequency around 40 kHz. Taking the phase shift in the stabilization system into consideration results in a build-up of the electron branch of the oscillations at densities below the threshold of hydrodynamic instability, which also is observed in the experiment. The behavior of the first radial mode is a little strange at densities above the threshold, where oscillations vanish, and the losses expected with the onset of instability do not appear (cf. Fig. 2). The reasons for the observed effects still are not clear. It is possible that with the appearance of hydrodynamic instability the radial distribution of density is changed, which is the reason for stability. The appropriate measurements of radial density distribution are not yet complete.

With high amplifications, when $1 - \left(\frac{a}{b}\right)^{2|m|} + K < 0$, in eq. (4) still another purely imaginary solution appears, corresponding to the surface wave. Equation (3) gives for the purely imaginary two neutral branches: an ionic with frequency greater than the precession frequency and rising with density, and an electronic propagated in the direction opposite ion drift. With advancing angular shift the electronic branch should be unstable, but a wave propagated opposite the direction of ion

drift was not observed in our experiments. The ionic branch was observed, but it had a more complex structure than follows from eq. (3). The behavior of the ionic branch can be explained, however, if it is correct to assume, as Varma suggests [11], the radial inhomogeneity of the magnetic field. For this, it is necessary to add a term to the right side of (3):

$$\beta \cdot \frac{\omega_{0i}^2}{\omega_{Bi}^2} \cdot \frac{2m^2\omega^*}{(\omega + m\omega^*)^2} \qquad (6)$$

When it is figured in, another ionic branch appears with a frequency slightly above the precession frequency. For purely imaginary $\varkappa a$ the interaction of the two ionic branches leads to hydrodynamic instability at low densities. The ionic branches separate and become neutrally stable with an increase in density. The results of the calculations with an accounting of term (6) and also the correction for the final value of the Larmor radius, which shift the curve slightly to the right without changing it qualitatively, are shown in Fig. 7. Branch III is hydrodynamically unstable. Branch IV – the extension of the ionic branch – is unstable with a delayed phase shift, and branch V – the extension of the Varma branch – is unstable with the advancing shift. These theoretical conclusions agree with the experiment: forcing of the frequency characteristic of the amplifier results in excitation of the Varma branch, and a steep drop in the frequency characteristic excites the ionic branch.

It should be noted that the precise values of the slope of branch III, the stability threshold, and the path of branches IV and V greatly depend on the value of $\varkappa a$ and various minor corrections. Therefore, in this frequency region we cannot expect such good correspondence as for asymptotic low-frequency solutions. But the overall character of the dispersion dependencies is described correctly.

VI. Conclusions

These experiments showed:

1. The previously observed [2-5] effects of decreased losses for positive feedback are non-linear.

2. Linear stability can be achieved with negative feedback and a sufficiently large number of stabilizing electrodes.

3. The theory accounting for the magnetic field gradient is a sufficiently good description of the observed oscillation branches.

4. The created feedback system permits simultaneous and independent stabilization of several spatial modes of flute oscillations.

5. Internal flute oscillations actually are observed in the presence of a feedback system, but with a 2-3-fold elevation in their threshold the losses associated with them are not detected. Further experiments are needed to elucidate the reasons for this phenomenon and its role with a density increment.

As a general conclusion relating not only to open traps, the results of these experiments permit the statement that feedbacks are a practical functional method that makes it possible to simultaneously stabilize at least several oscillation modes in the parameter region exceeding the stability threshold by an order of magnitude.

The suthors thank V. V. Arsenin and A. V. Timofeev for numerous consultations, I. N. Golovin for his constant attention and support of the work, Yu. M. Pustovoyt, V. F. Zubarev, and Ye. Kuzin for developing the pulsed molecular beam, and the members of the "Ogra" section for their aid in conducting the experiments.

References

[1] V. A. Arsenin and V. A. Chuyanov, Dokl. Akad. Nauk SSSR, 180, (5), 1078 (1968).

[2] V. V. Arsenin, V. A. Zhil'tsov, and V. A. Chuyanov, "Plasma physics and controlled nuclear fusion research" (Proc. 3rd IAEA Conference, Novosibirsk 1968), Vol. 2, p. 515, IAEA, Vienna, 1969.

[3] V. A. Chuyanov and E. Murphy, "Yadernyy sintez" (12), 177 (1972).

[4] V. A. Chuyanov and E. Murphy, "Pis. ZhETF," 13, 553.

[5] V. A. Chuyanov, V. Kh. Likhtenshteyn, D. A. Panov, V. A. Zhil'tsov, and A. G. Shcherbakov, "Proc. 6th European Conf. on Plasma Physics and Controlled Fusion," p. 243, Moscow, 1973.

[6] A. L. Bezbatchenko, V. Ye. Keylin, Ye. Yu. Klimenko, I. A. Kovalev, B. P. Maksimenko, Ye. A. Maslennikov, S. A. Novikov, D. A. Panov, and N. N. Semashko, Preprint IAE-2284, Moscow, 1973.

[7] A. A. Panasenkov and N. N. Semashko, ZhETF, (12), 2525 (1970).

[8] B. B. Kadomtsev, ZhETF, 40, 328 (1961).

[9] M. N. Rosenbluth, N. Rostoker, and N. A. Krall, Nuclear Fusion, 1962, Supplement, p. 143.

[10] A. B. Mikhaylovskiy, ZhETF, 43, 509 (1962).

[11] R. K. Varma, Nuclear Fusion, 7, 57 (1967).

Figure captions

Fig. 1. Block diagram of 12-electrode stabilizing system for flute instability with Fourier dimensional synthesis. To simplify the figure, the compensation system for spurious feedback between sensing elements and electrodes is not shown.

Fig. 2. Mean plasma density as a function of product of injected current times gas lifetime.
- ● - without stabilization,
- ○ - only stabilization of mode m = 1 switched on,
- ▲ - stabilization of modes m = 1 and m = 2 switched on,
- ★ - stabilization system switched on without mode separation.

Superscripts m = 1, m = 2, and m = 3 denote the thresholds of build-up of the corresponding azimuthal modes.

Fig. 3. Potential on plasma axis as a function of plasma density with positive feedback [⊕], negative feedback [▲], and without stabilization [●].

Fig. 4. Axial distribution of plasma density at different injection currents and negative feedback [○] and with positive feedback [●].

Fig. 5. Plasma density and oscillation frequency of mode m = 1 as functions of phase shift in stabilizing channel m = 1. Stabilizing channel m = 2 operates in optimum mode. Amplification factor in channel m = 1 is constant at 0.25 rel. units (cf. Fig. 6).

Fig. 6. Oscillation frequency of mode m = 1 as a function of amplification in stabilization channel m = 1. Angular shift 45°. For all values of amplification, except K = 0, density is constant at $4 \cdot 10^8$ cm^{-3}. For K = 0 density is $1.6 \cdot 10^8$ cm^{-3}.

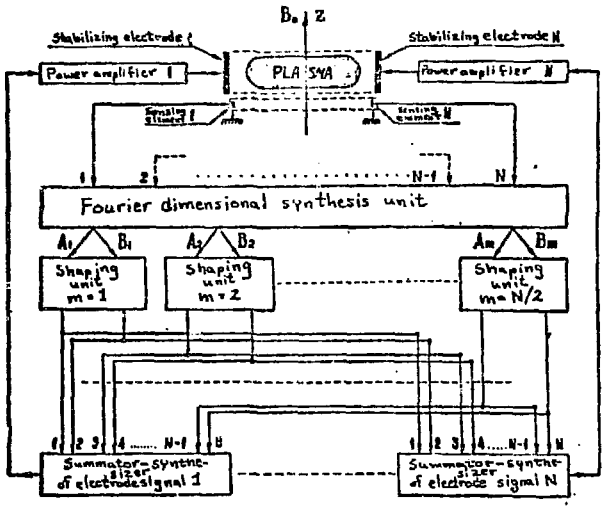
Stabilizing electrode 1
Stabilizing electrode N
Power amplifier 1
PLASMA
Power amplifier N
Fourier dimensional synthesis unit
Shaping unit m=1
Shaping unit m=2
Shaping unit m=N/2
Summator-synthesizer of electrode signal 1
Summator-synthesizer of electrode signal N

Fig. 1

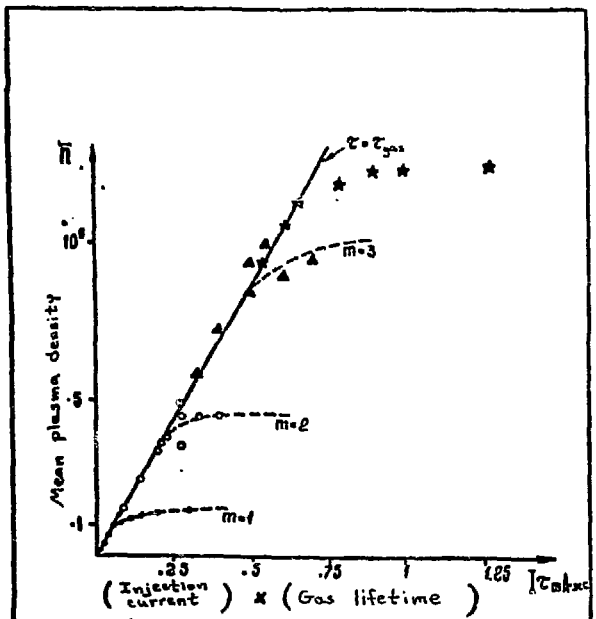
Mean plasma density
(Injection current) × (Gas lifetime)

Fig. 2

Fig. 7. Oscillation frequencies of mode m = 1 as functions of density. Experimental points are obtained during operation of stabilization channels m = 1 and m = 2. Amplification in channel m = 1 corresponds to 1 rel. unit in Fig. 6 and advancing angular shift of 45°. The sign ⟷ indicates the range of densities in which oscillations on the given frequency are observed. Amplitude peaks are denoted by ○ for internal and ▲ for surface waves. Theoretical curves are shown as solid lines. (I) dispersion curve of flute oscillations without feedback. (II) dispersion curve according to eq. (3) and (4) for K → ∞ for the first radial mode. The effect of the final Larmor radius of the ion is taken into account in the computations. Curve VI corresponds to the second radial mode with the same assumption as for curve II; curves III, IV, and V are obtained with an accounting of correction (6) and the effect of the final Larmor radius. They are computed for $\varkappa a = i \cdot 3.5$, which corresponds to the value of $\varkappa a$ obtained from (4) for amplification K = 1 rel. unit.

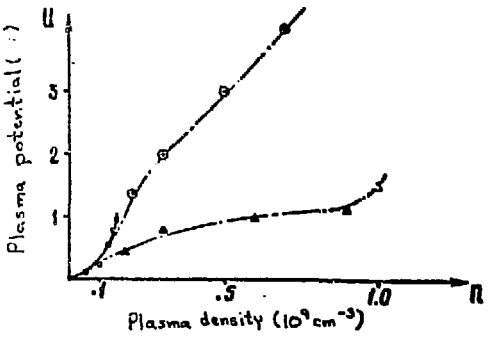
U
Plasma potential( )
3
2
1
.1
.5
1.0
n
Plasma density ($10^9 cm^{-3}$)

Fig. 3

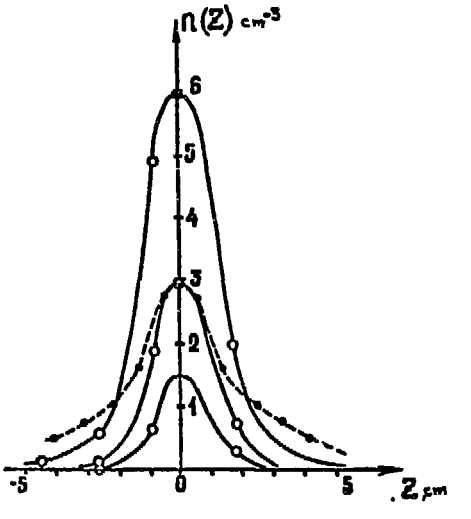
n(Z) cm^{-3}
6
5
4
3
2
1
-5
0
5
Z, cm

Fig. 4

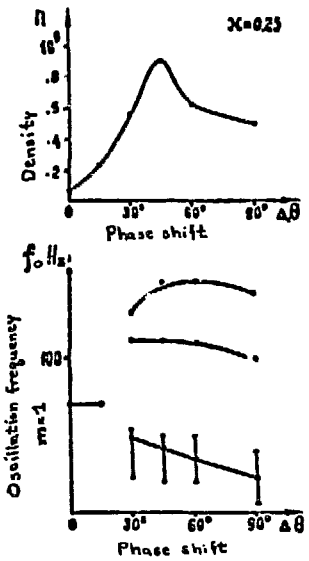
n
X=0.25
Density
Phase shift
Δθ
Oscillation frequency
m=1
Phase shift
Δθ

Fig. 5

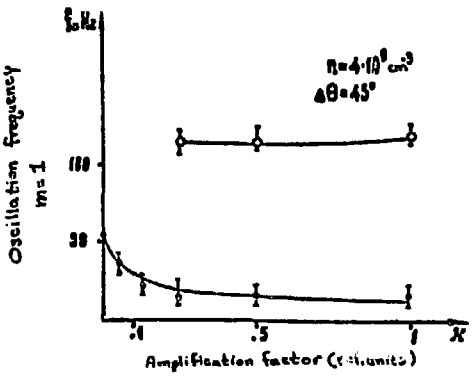
Oscillation frequency
m=1
n=4·10⁸ cm⁻³
Δθ=45°
Amplification factor (arb. units)
X

Fig. 6

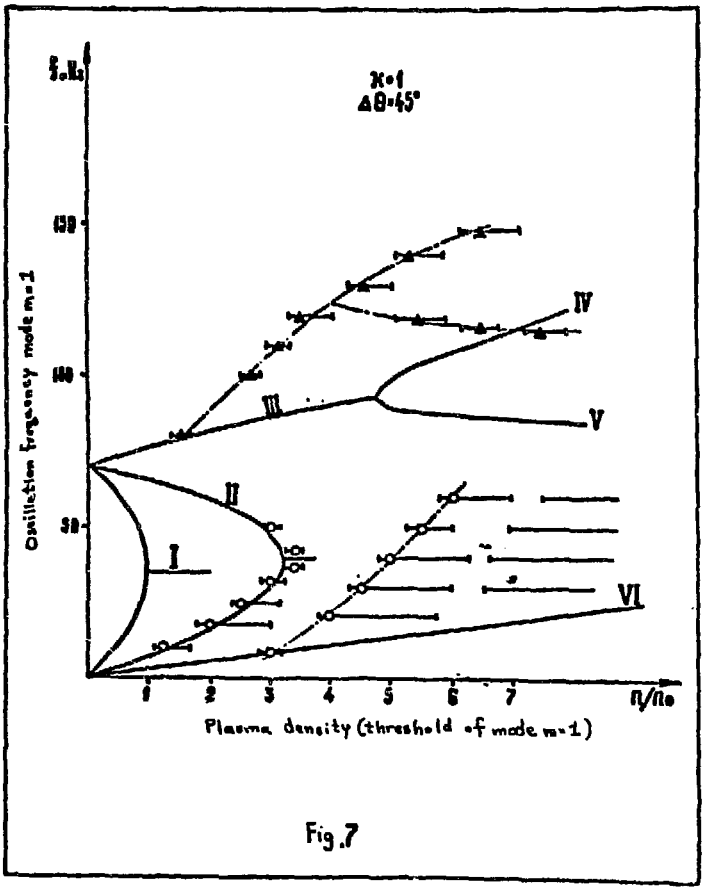
f, kHz
X=1
Δθ=45°
150
100
50
Oscillation frequency mode m=1
I
II
III
IV
V
VI
1
2
3
4
5
6
7
n/n₀
Plasma density (threshold of mode m=1)

Fig.7